Distributions of H-Bonding Aggregates in *tert*-Butyl Alcohol: The Pure Liquid and Its Alkane Mixtures

Paola Sassi,*,† Francesca Palombo,† Rosario Sergio Cataliotti,†,‡ Marco Paolantoni,† and Assunta Morresi†

Dipartimento di Chimica, Sezione di Chimica Fisica, Università di Perugia, Via Elce di Sotto 8, I-06123 Perugia, Italy, and Istituto Nazionale di Fisica della Materia, Unità di Catania, 95100 Catania, Italy

Received: February 27, 2007; In Final Form: May 8, 2007

A vibrational analysis using FTIR and Raman spectroscopies was carried out on pure liquid *t*-butyl alcohol (TBA) in the range of temperatures $15 \leq t \leq 70$ °C. The whole range of molar fractions for TBA in 2,2′dimethylbutane (2,2′DMB) was also explored and compared with the *t* dependence of pure alcohol properties. Temperature and composition dependence of vibrational spectra were reproduced by simultaneous fitting of IR and Raman OH-stretching band contours by using harmonic frequencies and intensities derived from *ab initio* calculations for the various hydrogen-bonded structures. Adopting this fitting procedure, size and shape distributions of H-bonding aggregates have been derived, thus giving a quantitative description of balancing factors between hydrophilic and hydrophobic interactions in this liquid system.

Introduction

Experimental evidence,[1−6] supported by theoretical and computational studies,[7−10] on the self-association properties of monohydric alcohols are available at present. In this context, *tert*-butyl alcohol (TBA) plays an important role because of the balancing of hydrophilic and hydrophobic properties in this molecular liquid. Despite its relatively large alkylic portion, TBA is completely soluble in both water and hydrocarbon solvents. This is due to its distinctive molecular structure that can be considered, together with that of methanol, the most symmetric structure among small monohydric alcohols. Unlike methanol, however, where the hydrophilic character strongly prevails over the hydrophobic one and a significant self-aggregation occurs via H-bonding (HB),[11,12] TBA has smaller H-bond clusters and a stronger hydrophobic character.

The molecular structure of this liquid has a strong effect on both the extension of the HB network and the geometric shape of its aggregates. The geometric shape of the hydrogen-bonded clusters in normal alcohols is prevalently a linear chain and involves many molecular units; however, a steric hindrance in proximity to the OH functionality (secondary and tertiary alcohols) tends to favor cyclic species.[6,12] The size of these species is usually limited by entropic effects.

A recent work from this laboratory[13] reports the effects of the nonideal mixing of TBA and 2,2′dimethylbutane (2,2′DMB) on the equilibrium and transport properties of the liquid mixture through the analysis of Brillouin spectra together with density and viscosity data. It was observed that changes in temperature and composition can have quite different effects on a series of hydrodynamic observables that are directly measured or derived. This is mainly due to two conflicting factors, namely, solute−solvent nonspecific interactions (van der Waals' forces) and solute−solute aggregation forces (hydrogen-bond connectivity). Their mutual balancing has a great effect on the structure of clusters because the polar OH group can be more or less exposed to the solvation shell depending on aggregate shape and size.

In such a HB system, the estimation of size distribution is very difficult because it is defined by a series of equilibrium constants for pseudo-consecutive reactions, which are not independent of one another.

The aim of the present article is to provide the aggregate distribution among the various HB species (HB populations) for liquid TBA by analyzing the vibrational spectra in the OH-stretching region. To this end, the components embodied in the IR and Raman OH-stretching contours were evaluated in order to get independent integrated intensities to be correlated with the population distributions, thus following and interpreting the temperature and solvation effects on the self-association properties of this liquid alcohol.

Experimental Procedures

The chemicals were all commercial products (>99.5% purity) obtained from Fluka and were used without any further purification.

Infrared spectra of TBA and its alkane solutions were measured using a FTIR model IFS113V Bruker spectrometer with a resolution of 1 cm^{-1} in the spectral region between 2600 and 4000 cm^{-1}. The measurements were executed at temperatures ranging from 15 to 70 °C, with a sample chamber pressure of ca. 3 mbar to avoid air humidity interference. A cell equipped with KRS5 windows was used, which had a high signal-to-noise ratio in the entire MIR range.

Raman spectra were recorded using an ISA Jobin-Yvon model U1000 double monochromator with 1 m focal length holographic gratings and photon counting detection. The exciting source was a Coherent model Innova 90 argon ion laser used in single-line excitation mode at 514.5 nm. The power focused on the samples was always less than 600 mW. The scattered Raman photons were detected using a thermoelectrically cooled Hamamatsu model 943XX photomultiplier, which, through a photon counting chain and an acquisition board system, is

* Corresponding author. E-mail: sassipa@unipg.it.
† Università di Perugia.
‡ Unità di Catania.

10.1021/jp071609q CCC: $37.00
Published on Web 06/19/2007

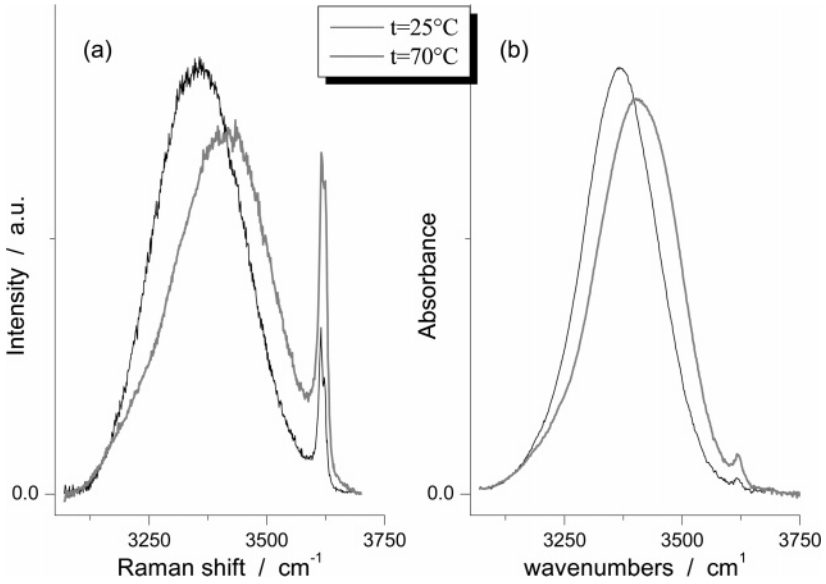

Figure 1. OH-stretching band contours of *tert*-butanol Raman (a) and IR (b) spectra.

computer-controlled by the ISA Jobin-Yvon SpectraMax package. The same software allows for automatic handling of the experiments, that is, acquisition of raw data and their manipulation. The spectra were recorded with vertical−vertical (VV) polarization scattering geometries by a timely set up of a Melles-Griot polarization rotator placed in front of the sample. Accurate focusing was obtained via micro-movements of XYZ micro-translators on which all of the entrance and collecting lenses were mounted. Accuracy of the Raman measurement is 1 cm^{-1}.

The temperature was controlled by circulating water from a Haake F6 ultra-thermostat, which permitted a precise temperature setting of ±0.1 °C. An electronic thermometer mounted in the measurement cells controlled the exact temperature values of the samples.

Results and Discussion

IR and Raman OH-Stretching Profiles. The temperature effect on Raman and IR OH-stretching ($\bar{\nu}_{OH}$) profiles of pure TBA is shown in Figure 1. Spectroscopic measurements were taken to explore the supercooled liquid in the 15−25 °C range and normal conditions up to 70 °C; a continuous evolution of spectral features was observed. All spectra were subtracted for CH-stretching signals, both fundamental and combination bands.[14] A marked blue shift of the broad *H-bonded* component (HBC), together with a strong intensification of the *free-OH* (FOH) band at ca. 3620 cm^{-1}, was clearly detected when the temperature increased.

In a previous study conducted by our group, the high-frequency FOH component of liquid TBA was analyzed and compared with analogous components of 1- and 2-octanol.[15] In 1- and 2-octanol, a doublet was present and was attributed to trans and gauche rotational isomers. The FOH Raman signal of pure TBA at room temperature is composed of two sub-bands, centered at 3614 and 3623 cm^{-1}. In this case, the rotational isomerism cannot be invoked to explain the spectral feature; consequently, the lower frequency sub-band is assigned to β OHs and the higher frequency one (3623 cm^{-1}) to α OHs. The β groups refer to proton-acceptor terminal hydroxyls; on the contrary, the α OHs are not involved with the H-atom nor with the oxygen lone pairs in H-bonding interactions and refer to monomeric TBA. Thus, the corresponding OH-vibrational mode is not affected by either intermolecular (H-bonding) or intramolecular (conformation) interactions. This result is very important because it suggests the possibility of using the IR and Raman spectra as direct probes of monomer species in such a liquid system. This cannot be done with primary and secondary alcohols because of the complex superposition of both the α−β and the trans−gauche signals. The analysis of the FOH band at room temperature shows the prevalence of β over α OHs, which indicates that a substantial degree of self-aggregation also exists in this tertiary alcohol.[15]

The effects of an increase in temperature on HBC and FOH band profiles is completely different from those observed on diluting the alcohol in 2,2′-dimethylbutane. In this case, as Figure 2 clearly shows, the *free-OH* band increases greatly when going from $x_{OH} = 1.0$ to $x_{OH} = 0.1$ (x_{OH} = alcohol molar fraction), and the H-*bonded* $\bar{\nu}_{OH}$ component shows a small (perhaps anomalous) red shift. In fact, the more the hydroxyl group is involved in the H-bonding network, the more its $\bar{\nu}_{OH}$ frequency is red-shifted; our data show an anomalous trend because the red shift is observed on diluting the alcohol in 2,2′DMB, and this is usually not expected. The results shown in Figure 2 support the idea that despite the large production of monomers, the effect of dilution does not cause a progressive reduction in cluster size as occurs when the temperature is increased.

A detailed description of the distributions in cluster dimensions can be achieved by proper analysis of $\bar{\nu}_{OH}$ IR and Raman profiles. In a recent study by Andanson et al.,[16] *ab initio* calculations at the HF/6−31 G* level were carried out in order to evaluate harmonic frequencies and IR and Raman intensities of the OH-stretching mode for the different TBA self-associating clusters. By using these band parameters, the profiles of *t*-butyl alcohol in supercritical (SC) conditions were decomposed in a sum of Gaussians. In this model the authors considered a distribution of small oligomers, from monomers (dominant species), which are particularly revealed by the Raman technique, up to tetramers; the analysis thus allowed a quantitative description of the supercritical state of TBA.

The situation described by $\bar{\nu}_{OH}$ of SC *t*-butyl alcohol is only similar to that of the liquid at TPS thermodynamic conditions to a certain extent. In the supercritical domain, the IR spectrum exhibits a broad band at ca. 3550 cm^{-1} accompanied by a narrow intense absorption at about 3630 cm^{-1}; the intensity of the total

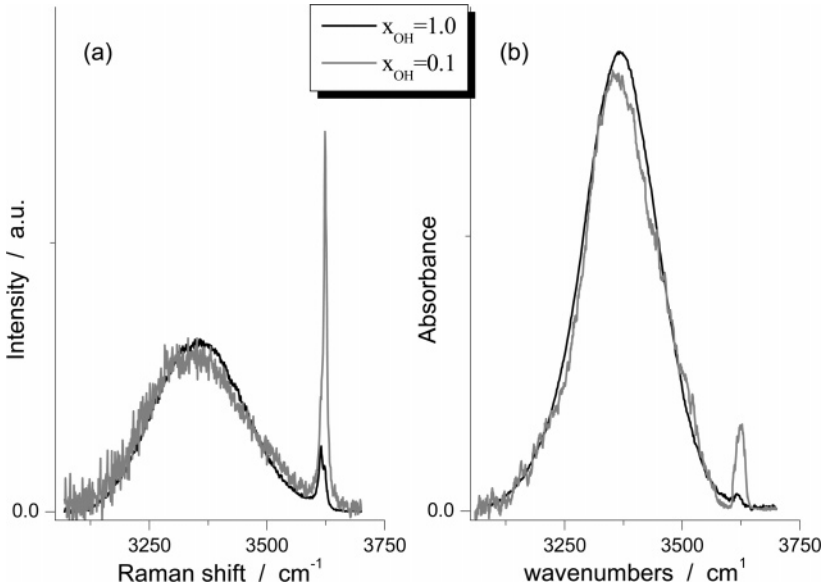

Figure 2. OH-stretching band contours of Raman (a) and IR (b) spectra for TBA-2,2′DMB solutions.

envelope vanishes completely below 3350 cm^{-1}. However, the OH-stretching IR profile of the liquid is completely red-shifted with a maximum in the 3350−3400 cm^{-1} region, which decreases to zero intensity at 3100 cm^{-1}. The different and broader extension of absorption clearly indicates the different self-associative conditions present in the liquid and SC states, with larger HB aggregates found in the liquid state. The same conclusion can be drawn when the Raman features are compared.

According to this simple qualitative spectral analysis, we believe that the decomposition of $\bar{\nu}_{OH}$ band, both Raman and IR, should include a larger number of components in normal liquid compared to that in SC spectra. In principle, such a treatment is inconvenient because the larger the number of parameters to be optimized, the less reliable the procedure. Therefore, we decided to simplify the problem by trying to select the types and shapes of oligomers to be included in the modeling. With this in mind, we collected the findings available in the literature. (1) The separation of α and β components in IR and Raman spectra of TBA allows a direct estimation of monomers and linear cluster populations (terminal $\bar{\nu}_{OH}$ oscillators) in the liquid phase.[15] (2) HB aggregates in tertiary alcohols in general and in *t*-butyl alcohol in particular are essentially cyclic.[17] (3) Owing to the high ring tension of the cyclic trimer, this species does not play a major role in TBA liquid structure and may be neglected.[1,16] (4) The cyclic *n*-mers of TBA are further stabilized if the coupled *tert*-butyl portions of the molecules show a cis−trans configuration with respect to the ring of H-bonded hydroxyls; this condition occurs when the cluster is made up of an even number of units.[1] (5) In addition to the energetic preference to form cyclic species, consideration has to be given to the fact that rings with a large number of alcohol molecules are not favored for entropic reasons.[18] (6) The SC domain of TBA is described as a function of monomer, linear dimer, and cyclic tetramer populations.[16] (7) MD simulations demonstrate that a cyclic tetramer is the dominant structural motif in the liquid state.[17] (8) X-ray diffraction data on liquid *t*-butyl alcohol strongly suggest the formation of hexamer ring clusters.[19]

Quantitative Band Shape Analysis. According to the above statements, we decided to model the structure of liquid *t*-butyl alcohol, a function of both temperature and dilution in 2,2′ DMB, as a distribution of monomers, linear dimers, cyclic tetramers, and cyclic hexamers. Such a picture of the liquid TBA system was also justified by previous findings from computational studies,[12,17] which indicated a sharp distribution of cyclic and linear aggregates, *n*-mers with $n < 10$, peaked at $n = 4$. With respect to the considered species, we used *ab initio* results of ref[16] and further deduced the frequency and activity data for the hexameric species (see below). We thus assumed that the Raman scattering $I(\bar{\nu}_{OH})$ and the infrared absorbance $A(\bar{\nu}_{OH})$ consist of a linear combination of sub-bands, Gaussian, or Lorentzian forms, weighted by the population coefficients and the Raman/infrared intensities of the corresponding OH modes. The population coefficient constitute the results of the fitting analysis, whereas the Raman/infrared intensities are fixed at their computed *ab initio* values and then taken frequency-independent over the width of each band. The curve-fit response for the decomposition of experimental OH-stretching vibrational profiles is expressed by the following equation:

$$I(\bar{\nu}_{OH}) \text{ (or } A(\bar{\nu}_{OH})) = n_1 I_{L1}\mathrm{L1}(\bar{\nu}_{OH}) + n_2 I_{L2}\mathrm{L2}(\bar{\nu}_{OH}) + n_2 I_{G2}\mathrm{G2}(\bar{\nu}_{OH}) + n_4 I_{G4}\mathrm{G4}(\bar{\nu}_{OH}) + n_6 I_{G6}\mathrm{G6}(\bar{\nu}_{OH}) \quad (1)$$

where n_i ($i = 1, 2, 4, 6$) is the population factor related to the *i*-size species, and I_{ji} ($j = \mathrm{L}, \mathrm{G}$) is the intensity (Raman or IR) of the *ji*-th component described by a Lorentzian (L) or Gaussian (G) function. $\mathrm{Li}(\bar{\nu}_{OH})$ and $\mathrm{Gi}(\bar{\nu}_{OH})$ contain the width and the frequency position of the band as fitting variables. Thus, as described by eq 1, we used Gaussian components (G4 and G6) for cyclic clusters, Lorentzian curve for monomers (L1), and one Lorentzian (L2) and one Gaussian (G2) functions for the linear dimer, in order to account for proton-accepting and -donating OH groups, respectively. The two OH-stretching oscillators of the dimeric cluster were separately taken into account because of the different effects of H-bonding interaction on OH-stretching frequency of proton-donor (γ OHs) and proton-acceptor (β OHs) hydroxyls.[15,20] A Lorentzian form was adopted in the modeling of α and β components considering the fact that these oscillators are less involved in intermolecular interactions. On the contrary, in the case in which the different involvement in H-bonding network (different local arrangement) produces a distribution of $\bar{\nu}_{OH}$ frequencies, one usually observes a Gaussian distribution of spectral intensities for this oscillator.[20(d)] Consequently, for the lower frequency components of the total $\bar{\nu}_{OH}$ profile, a Gaussian band shape was assumed in order to

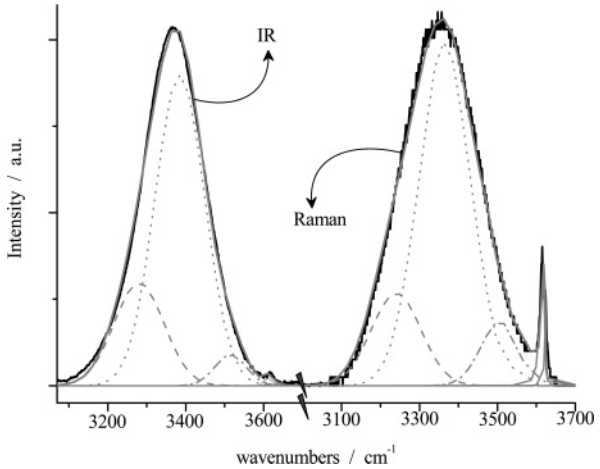

Figure 3. Results of curve fitting procedure on pure TBA ($t = 25$ °C). The fit is simultaneously performed on IR and Raman profiles.

account for the stronger H-bonding interactions giving an inhomogeneous frequency distribution.[16]

Under these assumptions, we simultaneously performed a decomposition of the IR and Raman OH-stretching spectra into distinct bands; this allowed the n_i parameters that best reproduce the observed features at a given concentration or temperature to be estimated. The close similarity between the IR absorption and I_{VV} Raman scattering responses in the spectral region of the fundamental OH-stretching vibrations should be noted. In this case, we fixed very precise limits for the variability of band position (± 5 cm^{-1}) and used fixed values of bandwidth and IR and Raman intensities, thus ensuring a better reliability of the final results according to the estimate of n_i values.

An example of band shape analysis of pure liquid at $t = 25$ °C is presented in Figure 3; the fit to both profiles showed a good agreement with experimental data, and Table 1 gives the resulting fitting parameters. The Figure also shows good agreement between the fitting curve and experimental data with the chosen components and parameters used. Such a decomposition of the very broad band at 3400 cm^{-1} (signature of HB aggregates) into three distinct components is very common for this kind of liquid[9,21,22] and is strongly suggested especially at high temperature and high dilution.[16,23,24] The difference in this case is that the three components refer to specific kinds of clusters; most of the literature data, on the contrary, refer to different oscillator classes.

Some differences can be noted between the values listed in Table 1 and those of the corresponding parameters found in SC *t*-butanol.[16] The band positions are slightly red-shifted to account for stronger interactions for the liquid alcohol under normal conditions; the components are wider in relation to a higher connectivity of the H-bonding network, which gives a larger inhomogeneous broadening of band profile.

In Table 1, the data for the monomer L1 band show the same IR and Raman position and width but different activities; the same is true for the linear dimer L2 and G2 bands. The G2 position is perfectly consistent with the analogue component of the IR spectrum of 1-hexanol in hexane.[23] As expected, the G2/L1 intensity ratio is much bigger for IR than Raman components because the intensity enhancement due to hydrogen bonding is much more effective in the absorption technique.[16]

The data of the cyclic tetrameric species show that the IR band position $(\bar{\nu}_{OH})_{IR}$ is slightly blu-shifted relative to the Raman position $(\bar{\nu}_{OH})_{Raman}$. The *ab initio* calculations of ref[16] clearly show that the sensitivities of the IR and Raman spectroscopies are different in the detection of the OH-stretching motion. In the case of a tetrameric aggregate, the authors indicate four different $\bar{\nu}_{OH}$ modes, and among these, the one at lower frequencies is not IR active. Consequently, the overall IR tetrameric intensity is blue-shifted with respect to the Raman signal. Regarding this species, we refer to a single class of oscillators that have a distribution that covers the whole range of tetrameric harmonic frequencies reported in ref[16] ($(\Gamma_{OH})_{IR} \approx (\Gamma_{OH})_{Raman} \approx 150$ cm^{-1}).

The blue-shift of our IR position observed for G4 was also found for the G6 component, and the explanation follows the arguments cited above. Unfortunately, the results of *ab initio* calculations are not available for the hexameric species that we introduced into the fitting procedure. Consequently, the values reported for this oligomer in Table 1 are those derived from the present analysis. The IR and Raman activities were extrapolated from the data from ref.[16] The intensities of the different contributions, from monomer to tetramer bands, were plotted as a function of their number of hydrogen bonds, and the trend was fitted by a second-order polynomial to account for the enhancement due to collective HB interactions; a good correlation was found ($R^2 = 0.983$). The IR and Raman activities of the hexameric cluster were extrapolated from this correlation. It is worth noting that this enhancement is particularly evident for IR and not so relevant for Raman intensities, and this is perfectly in line with previous findings.

One could argue that this procedure lacks a precise calculation of the band parameters and that it would be more reasonable to include a pentamer ring in the description of the liquid structure. Actually, *ab initio* calculations[18] on TBA ring clusters up to $n = 5$ alcohol units have shown that the difference in band position of tetrameric and pentameric cyclic structures is far below 100 cm^{-1}, the difference we found between the G4 and G6 subband positions. Also, with *ab initio* calculations, the average intermolecular bond length $r_{O\cdots O}$ in different molecular clusters of a simple alcohol, that is, ethanol, decreased with increasing cluster size up to $n = 4-5$.[25] These findings, confirmed by experimental NMR hydroxyl proton chemical shifts allow us to argue that the OH-stretching frequency should undergo an insignificant shift from tetramer to pentamer. This holds true for liquid ethanol and even more so for *t*-butanol, where the cis−trans configuration of even-membered aggregates further stabilizes the tetramer rings with respect to the pentamer despite the cooperative effect. The large width that we adopted for the two G4 and G6 components and their large superposition could be due to size distributions including the hidden $n = 5$ species but with maxima in $n = 4$ and $n = 6$.

TABLE 1: Parameters Used in Curve-Fitting Analysis of IR and Raman Profiles

HB specie		$(\bar{\nu}_{OH})_{IR}$ /cm^{-1}	$(\Gamma_{OH})_{IR}$ /cm^{-1}	I_{IR} /km mol^{-1}	$(\bar{\nu}_{OH})_{Raman}$ /cm^{-1}	$(\Gamma_{OH})_{Raman}$ /cm^{-1}	I_{Raman} /A^{4}amu^{-1}
cyclic hexamer (G6)		3290	150	4071.6	3240	150	646.9
cyclic tetramer (G4)		3410	150	1958.1	3380	160	446.9
linear dimer:	proton donor (G2)	3520	100	328.3	3520	100	130.7
	proton acceptor (L2)	3614	14	34.8	3614	14	54.5
monomer (L1)		3624	10	26.1	3624	10	71.4

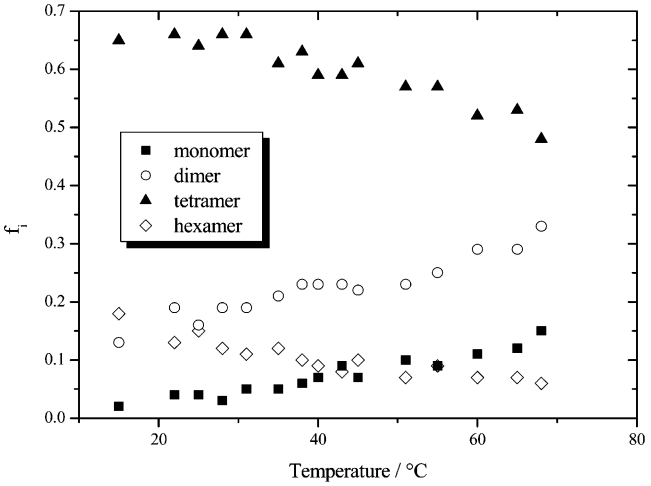

Figure 4. Temperature evolution of aggregate population fractions (f_i: see text) for pure TBA.

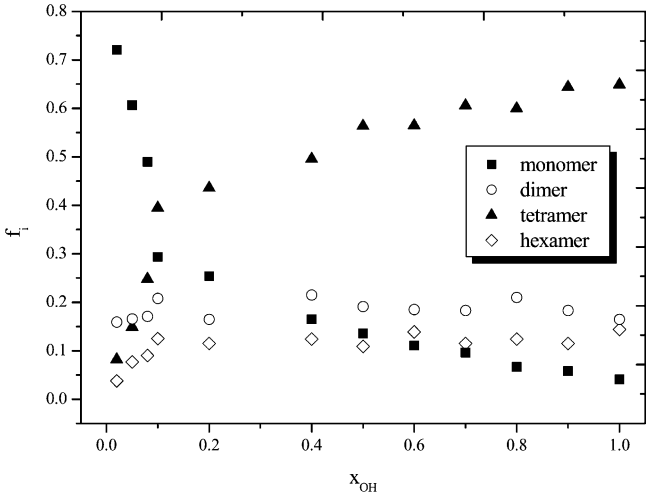

Figure 5. Composition dependence of aggregate population fractions for *t*-butyl alcohol in 2,2′dimethylbutane solution.

An additional argument to discuss for the assignment of $\bar{\nu}_{OH}$ IR and Raman sub-bands is in regards to the possible inclusion of linear structures. With respect to eq 1, it is possible to see that the population of the only linear aggregate (dimer) is responsible for both 3614(L2) and 3520(G2) cm^{-1} band intensities. Any other linear cluster should contribute to the intensity of the L2 band as well because this component is assigned to the terminal proton-accepting OH groups. Indeed, the frequency of the related stretching mode should not change considerably as the aggregate size increases. Our attempt to include other chain aggregates besides dimers (e.g., trimer or tetramer) definitely showed that the populations of these components were almost zero, especially at higher temperatures and low concentrations where the L2 band is clearly distinguished in both the IR and Raman spectra. Therefore, the kind of chain aggregates considered in the cluster distribution was limited to the dimeric species.

Oligomers in the *t*-Butyl Alcohol Liquid System. The fitting procedure described above allowed the n_1-n_6 populations for liquid TBA to be estimated. Figure 4 shows their evolution, in terms of fraction $f_i = n_i/\Sigma n_i$ in pure alcohol as a function of temperature. On the basis of these trends, a number of observations can be made. Tetrameric species predominate, with fewer hexamer, dimer, and monomer species present over the whole *t* range investigated. While tetramers are quite stable up to ca. 35 °C and then slowly decrease, the low percentage of hexamers decreases as temperature increases over the whole explored range. Moreover, the decrease of f_6 is more effective than f_4, as expected for a cluster with a larger formation enthalpy. However, increasing the temperature in the range of 15−70 °C decreased the tetramers and hexamers, while the monomer and dimer content increased. This result reflects the change of IR and Raman band profiles reported in Figure 1, where the intensification of the G4 and G6 bands upon cooling is explained by the overall red shift of HBC.

The n_1-n_6 distribution obtained by curve-fitting analysis can be used to estimate the concentrations of the different species; in turn, the formation enthalpy and entropy values for different molecular clusters can be evaluated. In particular, with reference to equations of the type $n\cdot M \leftrightarrow P_n$, where *M* is the monomeric alcohol species and P_n is the HB *n*-mer, one can define the equilibrium constant as $K_n = [P_n]/[M]^n$. From the temperature evolution of K_n values in pure liquid TBA, it is possible to obtain the formation entropy and enthalpy reported in Table 2 for different aggregates.

TABLE 2: Thermodynamic Quantities Derived by Concentrations of HB Aggregates

HB species	ΔH_f Kcal mol^{-1}	ΔS_f ue
cyclic hexamer	-46.4 ± 3.0	-129 ± 11
cyclic tetramer	-29.4 ± 1.8	-79 ± 7
linear dimer	-11.0 ± 0.8	-29 ± 3

An average strength of interaction of 7.3 and 7.7 kcal/mol of alcohol in tetramer and hexamer species, respectively can be deduced (Table 2). The slightly higher value obtained for the six-membered ring follows the effect of cooperativity foreseen for the H-bonding interactions. The ΔH_f value of the tetramer cluster is in line with the calorimetric studies on liquid alcohols; in contrast, the value obtained for the dimeric species is too high.[1,26] This is probably due to the fact that the intensities of the dimeric components (G2 and L2) are too low, especially at lower temperatures, and hence, their variation is not well estimated in our fitting procedure. This unexpectedly high ΔH_f value for the H-bonded dimer of liquid alcohols was also derived from the analysis of $\bar{\nu}_{OH}$ NIR spectra.[27] A possible explanation is that besides the limited accuracy of the techniques, the components that are usually assigned to the H-bonded dimer, both fundamental and overtone, could also include a contribution from the larger clusters (linear trimers).

Alcohol−Alkane Interactions. For the case of TBA in solution with 2,2′ DMB, the decomposition procedure described above was applied to analyze the IR and Raman profiles of the OH-stretching mode (the contribution of the alkane was previously subtracted from the spectrum). Fitting results in terms of f_i aggregate fractions are reported in Figure 5. Some considerations can be drawn from the comparison of these trends with those previously obtained for pure TBA as a function of *t* (Figure 4). As can be noted from the data in Figure 5, the tetramer retains its stability over the full composition range and is again the dominant aggregate. Diluting alcohol in alkane essentially affects the n_4 and n_1 populations, with a notable decrease of tetramers and a corresponding increase in the monomer fraction, and both tendencies increase at higher dilutions ($x_{OH} < 0.1$). In contrast, the f_6 and f_2 fractions are not really composition-dependent; their values remain basically constant over the $0.1 \leq x_{OH} \leq 1.0$ range. Consequently, the slight red shift of the HBC band maximum observed upon dilution as shown in Figure 2 cannot be due to the increase of

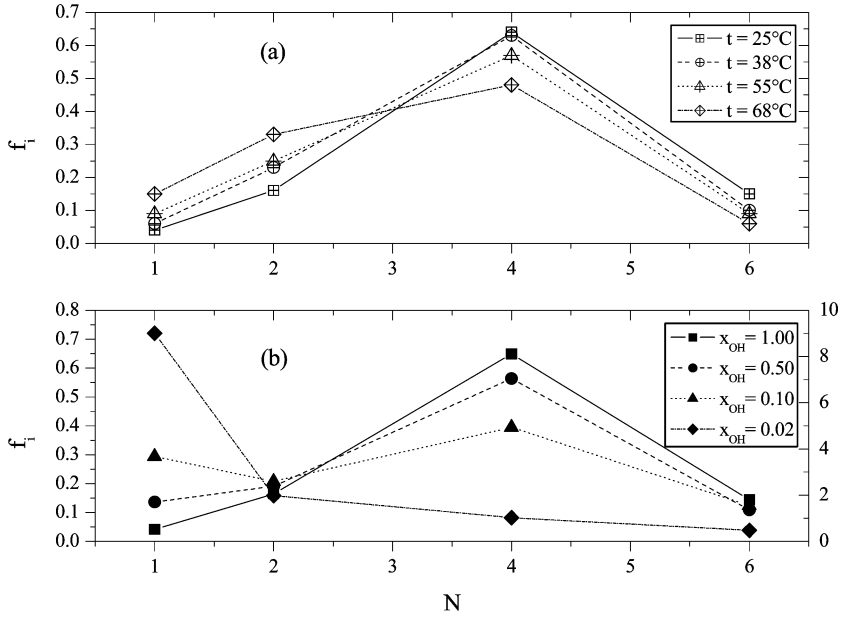

Figure 6. Population fractions of TBA H-bonded aggregates as a function of cluster dimension. (a) Pure alcohol at different temperatures. (b) TBA in 2,2′DMB at different x_{OH} molar fractions.

the largest aggregates but rather to the reduction of the dominant intermediate species.

This result is very important because it shows the substantial differences between temperature and dilution effects. These differences are notable with respect to the size distribution. As can be seen in Figure 6a when the temperature increases, the distribution of the populations progressively shifts to lower N values, where N is the number of molecules in the HB aggregate. On the contrary, when the molar fraction of alcohol in alkane solution is reduced, the content of medium-sized clusters decreases, while the amount of monomers increases (Figure 6b). Even at $x_{OH} = 0.1$, many TBA molecules are involved in self-aggregation, despite their low number per unit volume.

We recently reported density measurements on TBA-2,2′ DMB solutions as a function of temperature[13] and found the following relationship for the alcohol concentration c_{OH}:

$$c_{OH}(x)/\text{mol}\cdot\text{dm}^{-3} = 0.055 + 6.740x_{OH} + 3.740x_{OH}^{2} \quad (2)$$

for solutions having x_{OH} as TBA molar fraction at $t = 25$ °C. A relationship of the type

$$c_{OH}(t)/\text{mol}\cdot\text{dm}^{-3} = 10.900 - 0.012t \quad (3)$$

holds for pure liquid alcohol at temperature t (°C).

Thus, we decided to follow the evolution of populations of TBA clusters as a function of concentration ($c_{OH}(x)$ and $c_{OH}(t)$) in order to compare the effect of temperature and composition changes on liquid alcohol. Density was the pertinent parameter used to follow the effect of changing pressure in SC phase.[16] In the case of mixtures in a range where solute−solvent interactions are completely negligible, one could refer to the effects of dilution as a drastic reduction of alcohol concentration with a consequent reduction of self-association. In this sense, we compared the two situations: the one with pure liquid alcohol as a function of temperature on the one hand and that of the alcohol/2,2′ DMB mixture at different compositions on the other. Figure 7 displays the variation of the $\bar{N}$ average cluster dimension and the number n_{HB} of H-bonds per molecule obtained when the concentration was varied due to temperature (■) or composition change (○). These quantities are respectively defined by the following equations:

$$\bar{N} = (c_1 + 2c_2 + 4c_4 + 6c_6)/(c_1 + c_2 + c_4 + c_6) \quad (4)$$

$$n_{HB} = 2(0.5c_2 + c_4 + c_6)/(c_1 + c_2 + c_4 + c_6) \quad (5)$$

where c_1, c_2, c_4, and c_6 are the concentrations associated with the monomer, open dimer, cyclic tetramer, and hexamer of TBA, respectively, and c_i values are expressed as the product $c_i = n_i \cdot c_{OH}$. In eq 4, we introduced the monomeric species, thus considering $\bar{N} = 1$ as the lowest limit value of the average aggregate dimension, when the alcoholic system is only built upon monomers. The results obtained by using our computed aggregate populations n_i show that the clustering of TBA molecules is composition-dependent in such a way that both the average cluster dimension and the number of H-bonds per molecule tend to decrease with increasing dilution. Anyway, each quantity shows different trends above and below $x_{OH} = 0.1$ ($c_{OH} = 0.77$ mol dm^{-3}). A similar analysis was performed in TBA/CCl_4 solution by Iwahashi et al.;[28] the good agreement between the $\bar{N}$ values for TBA in two different solvents is quite surprising (Figure 7). It is known that carbon tetrachloride participates in weak interactions with free hydroxyls.[24,29] Nevertheless, the effects on TBA self-association seems to be more related to alcohol concentration than to specific solute−solvent interactions. Consequently, the average cluster dimensions follow the same trend in both apolar media.

We know that our alcohol−alkane mixture is not ideal.[13] The density, viscosity, and compressibility data account for this nonideality and suggest that the strength of attractive interaction among the molecules in solution is less than that in pure liquids. (Interactions between like molecules are more effective than those between different molecules.) A description of the alcoholic liquid structure at the microscopic level accounts for this behavior because it clearly shows how the alcohol aggregation in solution is less than that in pure liquid. Despite these weaker HB interactions, the trends of Figure 7 show another important aspect of the alcohol/alkane mixture: the average cluster dimension is quite large, even if the number of molecules

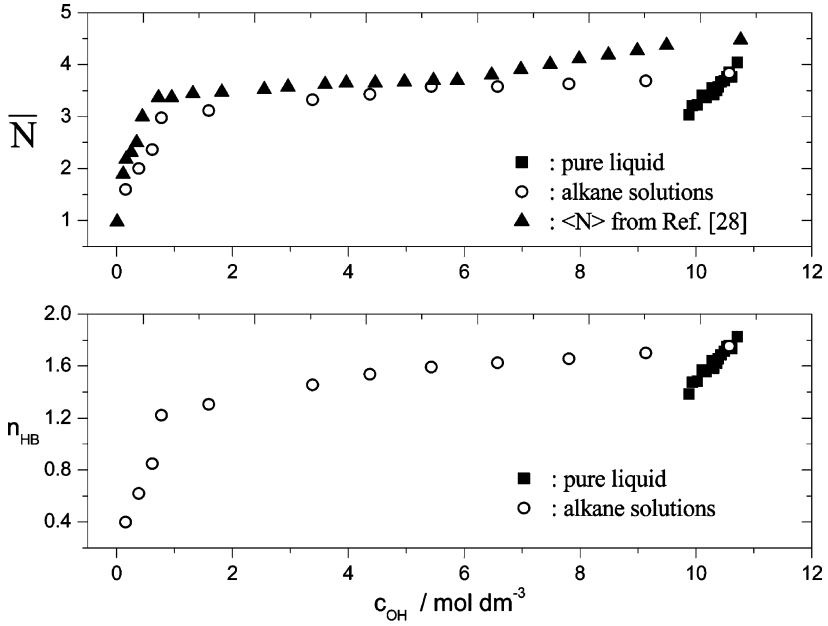

Figure 7. Average cluster dimension and number of H-bonds per molecule (see text) as a function of density: data for pure *t*-butyl alcohol (■) and for alcohol in alkane mixture (○). The average cluster dimensions evaluated in ref[28] for TBA/CCl_4 solutions (▲) is reported in the upper part of the Figure for comparison with present data.

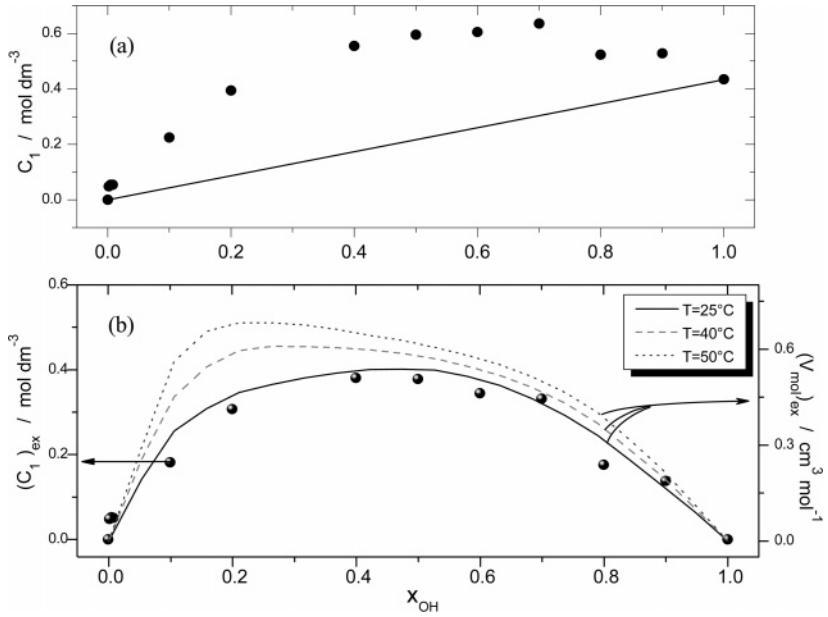

Figure 8. TBA/2,2′ DMB mixtures. (a) Concentration of monomer species as a function of alcohol molar fraction. Results of fitting procedure (●) and ideal behavior (—). (b) Difference $(c_1)_{ex}$ between experimental and ideal values of monomer concentration (●) and excess molar volumes of solutions (lines) as a function of alcohol molar fraction. The curves of excess molar volumes as a function of x_{OH} are evaluated from density measurements at temperatures 25 °C (—), 40 °C (---), and 50 °C (···).[13]

per unit volume is very small. Only when the TBA molar fraction is lower than 0.1 that there is a notable decrease in average size. In pure alcohol, however, a small density variation induced by a temperature decrease causes an appreciable decrease in the average dimension and, consequently, of n_{HB}. This result demonstrates that temperature has a stronger influence on the extent of aggregation in liquid TBA than dilution.

The qualitative reading of the IR and Raman profiles and band-shape analysis show that as a solvent 2,2′ DMB isolates alcohol molecules while still maintaining a certain degree of self-association, at least when $x_{OH} \geq 0.1$. This property of a liquid system is not surprising because it has also been observed in other alcohol−alkane mixtures,[9,21,30] and such a bimodal distribution with a large fraction of monomers in equilibrium with average-sized clusters is common in self-aggregating systems.[31−33]

Hydrophilic Solvation. The balance between the hydrophilic and hydrophobic character of this aliphatic alcohol causes the molecules to cluster in a way that reduces the exposure of *t*-butylic or OH functionalities to the aqueous or alkane environment, respectively. Analogous to the formation of direct micelle-like structures of TBA in water,[34,35] the diluted solutions of *t*-butanol in 2,2′ DMB could be an example of *inverse micelle-like* clustering. In this respect, an unusually high content of larger aggregates was observed even at lower alcohol concentrations.

The reason for this phenomenon can be described as follows. When assuming that liquid organic alcohols are built upon small

cyclic clusters, one would expect the organic groups to pack together as closely as possible in order to benefit from their van der Waals' interactions with hydrophobic solvents, whereas the OH groups should pack together by acting both as proton donors and proton acceptors. Most strikingly, such clusters would have a weaker dipole moment than monomers, and the interactions with their neighboring clusters in the liquid would be largely van der Waals' in nature.[1] In this way, the interactions of cyclic clusters with alkane molecules should be favored; on the contrary, the solvation of the hydroxylic portion of alcoholic monomers should not benefit from the van der Waals' interactions. This description accounts for the trends reported in Figure 7 and for the nonideal behavior described by the value of excess molar volumes of TBA-2,2′DMB solutions.[13] The concentration, c_1, of monomer species as a function of alcohol mole fraction is shown in the upper part of Figure 8. The straight line in Figure 8a represents the ideal behavior of a solution in which the concentration of monomers of pure liquid is scaled for TBA molar fraction in solution. The experimental c_1 values obtained from our fitting procedure were always higher than those expected for an ideal system. It should be noted that the L1 band intensity was the least affected by superposition with other components (especially in Raman spectra), and the extinction coefficient or Raman cross section was not dependent on the basis set of *ab initio* calculations. Consequently, the evaluation of f_1 is not critically dependent on fitting procedure. The differences $(c_1)_{ex}$ between experimental and ideal values at 25 °C are reported in Figure 8b (circles) together with the excess molar volumes $(V_{mol})_{ex}$ obtained at room temperature (solid black line) from our previous measurements. A perfect superposition between the trends of these two quantities is observed. The $(V_{mol})_{ex}$ values at different temperatures are also shown in Figure 8b; unfortunately, the $(c_1)_{ex}$ values are not available at $t = 40$ and 50 °C.

This result further supports our description of the structural properties of liquid TBA having higher polarity when the monomer content is higher. In this situation, a single TBA molecule is completely surrounded by solvent molecules or by the outer surface of cyclic HB structures; in particular, the hydroxylic portion is exposed to *t*-butyl groups of both the 2,2′DMB molecules and the TBA cyclic clusters.[15,36] Consequently, the solvation of monomers will correspond to a reduction of the overall van der Waals' interactions in proximity to the OH groups. Thus, the lower packing caused by this kind of interaction and the greater the average molar volume in solution. In this respect, the increase of $(V_{mol})_{ex}$ as the temperature increases is associated with the consistent amount of TBA monomers in solution, that is, higher over the whole concentration range, and particularly at lower x_{OH} values.

Conclusions

A vibrational analysis using FTIR and Raman spectroscopies was carried out on liquid *t*-butanol, over a wide range of temperatures and in the entire range of molar fractions in 2,2′dimethylbutane. The aim of the analysis was to determine any structural changes in the local hydrogen-bonding network of liquid alcohol, giving a quantitative description of the size distributions in pure liquid and alkane solutions. According to the data available in the literature, a limited number of different kinds of aggregates was considered, and the effects of temperature and dilution were described as a function of the distribution of monomers, open dimers, cyclic tetramers, and cyclic hexamers. A molecular description of the effect of hydrophilic solvation has been given and the origin of unfavorable alcohol−alkane interactions proposed.

References and Notes

(1) Benson, S. W. *J. Am. Chem. Soc.* **1996**, *118*, 10645.
(2) Hoffmann, M. M.; Conradi, M. S. *J. Am. Chem. Soc.* **1997**, *119*, 3811.
(3) Yamaguchi, T.; Benmore, C. J.; Soper, A. K. *J. Chem. Phys.* **2000**, *112*, 8976.
(4) Schwerdtfeger, S.; Köhler, F.; Pottel, R.; Kaatze, U. *J. Chem. Phys.* **2001**, *115*, 4186.
(5) van der Spoel, D.; van Maaren, P. J.; Larsson, P.; Timneanu, N. *J. Phys. Chem. B* **2006**, *110*, 4393.
(6) Palombo, F.; Sassi, P.; Paolantoni, M.; Morresi, A.; Cataliotti, R. S. *J. Phys. Chem. B* **2006**, *110*, 18017, and references cited therein.
(7) Sum, A. K.; Sandler, S. I. *J. Phys. Chem. A* **2000**, *104*, 1121.
(8) Kusalik, P. G.; Lyubartsev, A. P.; Bergman, D. L.; Laaksonen, A. *J. Phys. Chem. B* **2000**, *104*, 9526.
(9) Stubbs, J. M.; Siepmann, J. I. *J. Phys. Chem. B* **2002**, *106*, 3968.
(10) Stubbs, J. M.; Siepmann, J. I. *J. Am. Chem. Soc.* **2005**, *127*, 4722.
(11) Hoffmann, M. M.; Conradi, M. S. *J. Phys. Chem. B* **1998**, *102*, 263.
(12) Chen, B.; Potoff, J. J.; Siepmann, J. I. *J. Phys. Chem. B* **2001**, *105*, 3093.
(13) Cataliotti, R. S.; Palombo, F.; Paolantoni, M.; Sassi, P.; Raudino, A. *J. Chem. Phys.* **2007**, *126*, 44505.
(14) Korppi-Tommola, J. *Spectrochim. Acta, Part A* **1978**, *34*, 1077.
(15) Palombo, F.; Paolantoni, M.; Sassi, P.; Morresi, A.; Cataliotti, R. S. *J. Mol. Liq.* **2006**, *125*, 139.
(16) Andanson, J.-M.; Soetens, J.-C.; Tassaing, T.; Besnard, M. *J. Chem. Phys.* **2004**, *122*, 174512.
(17) Yonker, C. R.; Wallen, S. L.; Palmer, B. J.; Garret, B. C. *J. Phys. Chem. A* **1997**, *101*, 9564.
(18) Zimmermann, D.; Häber, T.; Schaal, H.; Suhm, M. A. *Mol. Phys.* **2001**, *99*, 413.
(19) Karmakar, A. K.; Sarkar, S.; Joarder, R. N. *J. Phys. Chem.* **1995**, *99*, 16501.
(20) (a) Wourtersen, S.; Emmerichs, U.; Bakker, H. J. *J. Chem. Phys.* **1997**, *107*, 1483. (b) Levinger, N. E.; Davis, P. H.; Fayer, M. D. *J. Chem. Phys.* **2001**, *115*, 9352. (c) Gaffney, K. J.; Davis, P. H.; Piletic, I. R.; Levinger, N. E. *J. Phys. Chem. A* **2002**, *106*, 12012. (d) Mc Hale, J. L. *Molecular Spectroscopy*; Prentice Hall Inc.: Upper Saddle River, NJ, 1999; Chapter 6.
(21) Murdoch, K. M.; Ferris, T. D.; Wright, J. C.; Farrar, T. C. *J. Chem. Phys.* **2006**, *116*, 5717.
(22) D'Aprano, A.; Donato, D. I.; Migliardo, P.; Aliotta, F.; Vasi, C. *Phys. Chem. Liq.* **1988**, *17*, 279.
(23) Gupta, R. B.; Brinkley, R. L. *AIChE J.* **1998**, *44*, 207.
(24) Sassi, P.; Morresi, A.; Paolantoni, M.; Cataliotti, R. S. *J. Mol. Liq.* **2002**, *363*, 96−97.
(25) Huelsekopf, M.; Ludwig, R. *J. Mol. Liq.* **2000**, *85*, 105.
(26) Solomonov, B. N.; Novikov, V. B.; Varfolomeev, M. A.; Klimovitskii, A. E. *J. Phys. Org. Chem.* **2005**, *18*, 1132.
(27) Ohta, A.; Murakami, R.; Urata, A.; Asakawa, T.; Miyagishi, S.; Aratono, M. *J. Phys. Chem. B* **2003**, *107*, 11502.
(28) Iwahashi, M.; Suzuki, M.; Katayama, N.; Matsuzawa, H.; Czaenecki, M. A.; Ozaki, Y.; Wakisaka, A. *Appl. Spectrosc.* **2000**, *54*, 268.
(29) Fletcher, A. N. *J. Phys. Chem.* **1969**, *73*, 2217.
(30) Paolantoni, M.; Sassi, P.; Morresi, A.; Cataliotti, R. S. *Chem. Phys.* **2005**, *310*, 169.
(31) DeBolt, S. E.; Kollman, P. A. *J. Am. Chem. Soc.* **1995**, *117*, 5316.
(32) McCallum, J. L.; Tieleman, D. P. *J. Am. Chem. Soc.* **2002**, *124*, 15085.
(33) Raudino, A.; Cataliotti, R. S.; Palombo, F.; Paolantoni, M.; Sassi, P., unpublished work.
(34) Kiselev, M.; Ivlev, D. *J. Mol. Liq.* **2004**, *110*, 193.
(35) Calandrini, V.; Deriu, A.; Onori, G.; Lechner, R. E.; Pieper, J. *J. Chem. Phys.* **2004**, *120*, 4759.
(36) Larsen, G.; Ismail, Z. K. *J. Solution Chem.* **1998**, *27*, 901.